# IMAGE SEGMENTATION BY COMBINING THE STRENGTHS OF RELATIVE FUZZY CONNECTEDNESS AND GRAPH CUT

*Krzysztof Chris Ciesielski,*[a,b] *P.A.V. Miranda,*[c] *Jayaram K. Udupa,*[b] *and A.X. Falcão*[d]

[a]Department of Mathematics, West Virginia University, Morgantown, WV 26506-6310

[b]Department of Radiology, MIPG, University of Pennsylvania, Blockley Hall – 4th Floor, 423 Guardian Drive, Philadelphia, PA 19104-6021

[c]Department of Computer Science, IME, University of São Paulo (USP), São Paulo, SP, Brazil

[d]Institute of Computing, University of Campinas, Campinas, SP, Brazil

## ABSTRACT

We introduce an image segmentation algorithm $\mathrm{GC}^{\max}_{\mathrm{sum}}$, which combines, in a novel manner, the strengths of two popular algorithms: Relative Fuzzy Connectedness (RFC) and (standard) Graph Cut (GC). We show, both theoretically and experimentally, that $\mathrm{GC}^{\max}_{\mathrm{sum}}$ preserves robustness of RFC with respect to the seed choice (thus, avoiding "shrinking problem" of GC), while keeping GC's bigger control over "leaking though the weak boundary." The theoretical analysis of $\mathrm{GC}^{\max}_{\mathrm{sum}}$ is greatly facilitated by our recent theoretical results that RFC belongs to the Generalized GC (GGC) segmentation algorithms framework. In our implementation of $\mathrm{GC}^{\max}_{\mathrm{sum}}$ we use, as a subroutine, a version of RFC algorithm (based on Image Foresting Transform) that runs (provably) in linear time with respect to the image size. This results in $\mathrm{GC}^{\max}_{\mathrm{sum}}$ running in a time close to linear.

***Index Terms*—** image segmentation, robustness, fuzzy connectedness, graph cut

## 1. INTRODUCTION

The algorithm we present in this paper belongs to the group of purely image-based (pI) segmentation algorithms (see e.g. [3, 10, 2, 9]), whose outputs are based entirely on the information available in the given image. Since the top-rated pI algorithms harness the information with equal effectiveness, there must exists similarity or even equivalence among such algorithms. This observation prompted researchers to study the possibility of explaining such algorithms in a common framework [1, 4]. In the same spirit, the popular graph cut (GC) framework has been generalized recently to, what we refer to as, *Generalized GC* (GGC). This framework was proposed by the authors in [5, 6], and studied in a slightly different form in [7], to describe GC, fuzzy connectedness (FC), and watershed (WS) algorithms in a unified manner. A byproduct of such a unification effort is a deeper understanding of the strengths and weaknesses of the individual algorithms, which can lead to new methods with improved performance, as we will demonstrate in this paper.

In this work, which falls within the GGC [5, 6] realm, we identify and justify some of the strong and weak properties of GC and FC, both theoretically and empirically, in a comparative manner. The most crucial among these are robustness of segmentation with respect to the selection of seed points (FC better than GC), boundary smoothness (GC better than FC), and computational efficiency (FC better than GC). The proposed new algorithm combines the best of both GC and FC and achieves an intermediate speed close to that of FC.

## 2. GENERALIZED GRAPH CUT FRAMEWORK

In every algorithm within GGC, a digital image $I = \langle C, f\rangle$ (where $C$ is its *domain* and $f\colon C \to \mathbb{R}^\ell$ its *intensity function*) is identified with a weighted directed graph $G = \langle V, E, w\rangle$ such that: (1) $V$ is the set of vertices of the graph and is equal to the image domain $C$. (2) $E$ is the image scene adjacency relation. In particular, $E \subset V \times V$ is a binary relation representing the set of all directed edges of $G$, that is, $\langle c, d\rangle$ is an edge if, and only if, $\langle c, d\rangle \in E$. It is assumed that $E$ is symmetric, that is, $\langle d, c\rangle$ is an edge provided so is $\langle c, d\rangle$. (3) $w\colon E \to [0, \infty)$ is a weight function associating with any edge $e \in E$ its weight $w(e)$. It is assumed that $w$ is symmetric: $w(c, d) = w(d, c)$ for every edge $\langle c, d\rangle$.

For every weighted graph $G = \langle V, E, w\rangle$, consider the space $\tilde{\mathcal{X}}$ of all functions $x\colon V \to [0, 1]$, referred to as *fuzzy subsets* of $V$, with the value $x(c)$ indicating a degree of membership with which $c$ belongs to the set. The family $\mathcal{X}$ of all functions $x \in \tilde{\mathcal{X}}$ with the only allowed values of 0 and 1 (i.e., $x\colon V \to \{0, 1\}$) will be referred to as the family of all *hard subsets* of $V$. Each $x \in \mathcal{X}$ is identified with the true subset $P = \{c \in V\colon x(c) = 1\}$ of $V$. Notice that, in such a case, $x$ is the *characteristic function* $\chi_P$ of $P \subset V$. In this paper we will consider only the space $\mathcal{X}$. The fuzzy sets $x \in \tilde{\mathcal{X}}$ in GGC are the subject of [7] and discussed in detail in [6].

The goal of the segmentation algorithms is to indicate, in the input image $I = \langle C, f\rangle$, a "desired" object $P \subset C$, which is identified with its characteristic function $\chi_P \in \mathcal{X}$. We usually restrict the collection $\mathcal{X}$ of all allowable "desir-

able" objects by indicating two disjoint sets, referred to as *seeds*: $S \subset C$ indicating the object and $T \subset C$ indicating the background. This restricts the collection of allowable outputs of the algorithms to the family $\mathcal{X}(S,T)$ of all $x \in \mathcal{X}$ with $x(s) = 1$ and $x(t) = 0$ for all $s \in S$ and $t \in T$. Note that $\mathcal{X}(S,T) = \{\chi_P \colon S \subset P \subset C \setminus T\}$.

For $q \in [1,\infty]$ consider the energy functional $\varepsilon_q \colon \tilde{\mathcal{X}} \to [0,\infty)$, where, for every $x \in \tilde{\mathcal{X}}$, $\varepsilon_q(x)$ is defined as the $q$-norm of the functional $F_x \colon E \to \mathbb{R}$, given by a formula $F_x(c,d) = w(c,d)|x(c) - x(d)|$ for $\langle c,d\rangle \in E$. That is,

$$\varepsilon_\infty(x) = ||F_x||_\infty = \max_{\langle c,d\rangle \in E} w(c,d)|x(c) - x(d)|,$$

$$\varepsilon_q(x) = ||F_x||_q = \sqrt[q]{\sum_{\langle c,d\rangle \in E} \big(w(c,d)|x(c) - x(d)|\big)^q}$$

for $q < \infty$. Notice that $\lim_{q\to\infty} \varepsilon_q(x) = \varepsilon_\infty(x)$, since $q$-norms converge, as $q \to \infty$, to the $\infty$-norm. We will use these functionals mainly for $x = \chi_P \in \mathcal{X}$. In this case, if $\mathrm{bd}(P)$ is defined as the set of all edges $e = \langle c,d\rangle$ with $x(c) \neq x(d)$, then $\varepsilon_q(\chi_P) = \sqrt[q]{\sum_{\langle c,d\rangle \in \mathrm{bd}(P)} \big(w(c,d)\big)^q}$ and $\varepsilon_\infty(\chi_P) = \max_{\langle c,d\rangle \in \mathrm{bd}(P)} w(c,d)$.

For $1 \leq q \leq \infty$, graph $G = \langle V,E,w\rangle$ (associated with $I = \langle C,f\rangle$), and seed sets $S$ and $T$, let $\varepsilon^q_{\min}$ be the minimum of the energy $\varepsilon_q(x)$ over all $ST$-allowable objects $x \in \mathcal{X}(S,T)$, that is, $\varepsilon^q_{\min} = \min\{\varepsilon_q(x) \colon x \in \mathcal{X}(S,T)\}$. Any element of $\mathcal{X}_q(S,T) = \{x \in \mathcal{X}(S,T) \colon \varepsilon_q(x) = \varepsilon^q_{\min}\}$ will be referred to as an energy $\varepsilon_q$ minimizer of $\mathcal{X}(S,T)$. Any algorithm $A$ that, given an image $I$ and seed sets $S$ and $T$, returns an object, denoted as $A(I,S,T)$, from $\mathcal{X}_q(S,T)$ will be referred to as an *$\varepsilon_q$-minimizing algorithm*. Notice, that any such algorithm has also a hidden aspect: a subroutine, denote it $I \mapsto w$, that translates the input image $I$ into its associated graph $G = \langle V,E,w\rangle$. We will write $A_{I\mapsto w}$ in place of $A$ if we like to stress this parameter.

Notice that the standard min-cut/max-flow algorithm is an $\varepsilon_1$-minimizing algorithm. We will use a symbol $\mathrm{GC}_{\mathrm{sum}}$ to denote this algorithm. We have recently proved [5, 6] that both *Relative Fuzzy Connectedness, RFC,* and *Iterative Relative Fuzzy Connectedness, IRFC*, algorithms are the $\varepsilon_\infty$-minimizing algorithms. Moreover, we proposed in [6] an IRFC segmentation algorithm, $\mathrm{GC}_{\max}$, based on the Optimum Path Forest Framework [8], and proved that it runs in linear time with respect to the image size.

For $1 < q < \infty$, the $\varepsilon_q$-minimizing algorithms cannot bring anything truly new to this picture, since any $\varepsilon_q$-minimizing algorithm $A_{I\mapsto w}$ is also an $\varepsilon_1$-minimizing algorithm $A_{I\mapsto w^q}$. This is so, since for both these algorithms the associated sets $\mathcal{X}_q$ and $\mathcal{X}_1$ are identical.

The $\varepsilon_1$- and $\varepsilon_\infty$-minimization problems (and so, the associated algorithms) are truly distinct, as discussed in [5, 6]. Nevertheless, there is an interesting connection between them, as proved in [6]: for every image $I$ there exists a $q < \infty$ such that the family $\mathcal{X}_1(S,T)$ associated with any $\varepsilon_1$-minimizing algorithm $A_{I\mapsto w^q}$ (e.g., for $A = \mathrm{GC}_{\mathrm{sum}}$) is contained in the family $\mathcal{X}_\infty(S,T)$. In particular, the output of $A_{I\mapsto w^q}$ minimizes $\varepsilon_\infty$ in $\mathcal{X}(S,T)$ and, in the case when $\mathcal{X}_\infty(S,T)$ has only one element, $A_{I\mapsto w^q}(I,S,T) = \mathrm{GC}_{\max}(I,S,T)$.

## 3. THE NEW ALGORITHM

The $\varepsilon_1$- and $\varepsilon_\infty$-minimizing algorithms, $\mathrm{GC}_{\mathrm{sum}}$ and $\mathrm{GC}_{\max}$, have their complementary strengths and weaknesses [5, 6]. From the point of view of this paper, the most important differences between these algorithms lie in the sensitivity of their output to the choice of the seed sets and the nature of the object's boundary in the input image. Specifically, the outcome of the $\varepsilon_\infty$-minimizing algorithms, $\mathrm{GC}_{\max}$, as well as its older versions RFC and IRFC, is *completely unaffected* by any changes of the seed sets within the delineated object. (See Thm 3.1 below.) In particular, relatively small sets of seeds, chosen with little care, often lead to the same output as carefully chosen seeds. However, the output of the $\varepsilon_\infty$-minimizing algorithms is independent of the object boundary size. So, their output has a greater chance of being jerky and/or passing through weakly visible segments of the true object boundary, as can be seen in Figure 1(b,d,e).

On the other hand, the $\varepsilon_1$-minimizing algorithms, including $\mathrm{GC}_{\mathrm{sum}}$, have a tendency to choose the objects with small boundary. This behavior, known as a shrinking problem[1], is especially acute, when the sets of seeds are small, in which case the algorithm has a tendency to output, as a delineated object, a small set very close to the set of object-indicating seeds, see, e.g., Figure 1(c). However, this is not an issue, when the input seed sets are relatively big, especially, when they are relatively close to the desired object and background. At the same time, the tendency of choosing the objects with small boundaries decreases the chance that an output object crosses a true, weakly visible boundary, consequently reducing the likelihood of causing delineation errors, usually referred to as leaking problems. Moreover, this decreasing of boundary size has a boundary smoothing effect, a feature that may be desirable for many image segmentation tasks.

To combine the strengths of both kinds of minimization strategies, we devised the following algorithm. Basically, we obtain a first approximation of the object by applying the most conservative $\mathrm{GC}_{\max}$ algorithm; we obtain the final delineation by applying $\mathrm{GC}_{\mathrm{sum}}$ to the output of thus created first approximation. The first step increases (possibly small) sets of seeds, preserving the algorithm's robustness (with respect to seed choice) and avoiding the shrinking problem of $\mathrm{GC}_{\mathrm{sum}}$, see Figure 1(d,e). The second step refines this approximation by enlarging it to an object with a smoother boundary, see Figure 1(f). This final increase creates only a small risk of

[1]The shrinking problem has been addressed by many authors, via modifications of the GC method, such as the normalized cuts. However, finding the resulting delineation minimizing normalized cut energy measure is NP-hard and so only approximate solutions can be found in practical time.

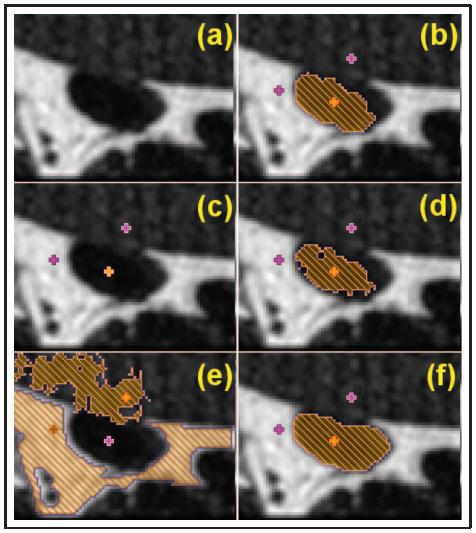


**Fig. 1**. (a) A 2D medical image of a vessel. (b) IRFC result object using 8-neighborhood with the cost function $w(p,q) = K - |I(p) - I(q)|$. (c) $\mathrm{GC}_{\mathrm{sum}}$ object, used with $w$, collapses the object to the seeds. (d) RFC object $\hat{S}$, for the internal seeds. (e) RFC object $\hat{T}$, for the external seeds. (f) The $\mathrm{GC}_{\mathrm{sum}}^{\mathrm{max}}$ returned object, resulting from applying $\mathrm{GC}_{\mathrm{sum}}$ to seed sets $\hat{S}$ (from (d)) and $\hat{T}$ (from (e)).

object leaking, the attribute of $\mathrm{GC}_{\mathrm{sum}}$. More specifically, the new algorithm is as follows.

**Algorithm** $\mathrm{GC}_{\mathrm{sum}}^{\mathrm{max}}$
**Input:** Image $I = \langle C, f\rangle$, non-empty seed sets $S, T \subset C$.
**Output:** An object $\chi_P$ from $\mathcal{X}(S,T)$.

1. create graph $G = \langle V, E, w\rangle$ associated with $I$;
2. use the RFC version of $\mathrm{GC}_{\mathrm{max}}$ on $G$ twice
   to find: the smallest $\hat{S}$ with $\chi_{\hat{S}} \in \mathcal{X}_\infty(S,T)$
   and the smallest $\hat{T}$ with $\chi_{\hat{T}} \in \mathcal{X}_\infty(T,S)$;
3. apply $\mathrm{GC}_{\mathrm{sum}}$ to $G$ and seeds $\hat{S}$ and $\hat{T}$ to find $\chi_P$;
4. return $\chi_P$;

The fact that both algorithms, $\mathrm{GC}_{\mathrm{max}}$ and $\mathrm{GC}_{\mathrm{sum}}$, can use the same weighted graph $G$, associated with the input image $I$, makes the merging of these two algorithms effortless.

Line 1 of the algorithm constitutes a "hidden parameter" of the algorithm, as mentioned above. The choice of the weight function, which in FC literature is called the *affinity* function, is explained in more detail in the next section.

Line 3 is straightforward: the modified sets $\hat{S}$ and $\hat{T}$ of seeds, provided by the $\mathrm{GC}_{\mathrm{max}}$ step, are already quite large and close to the desired object, there is little danger for shrinking. Also, $\mathrm{GC}_{\mathrm{sum}}$ has a smoothing effect on the final output.

Line 2 requires few words of explanation. To find $\hat{S}$, we run $\mathrm{GC}_{\mathrm{max}}$ in a version described in [6, sec. 4.3] which, in particular, returns a function $\mu^C(\cdot, W)$ from $C = V$ into $[0,1]$. We run $\mathrm{GC}_{\mathrm{max}}$ twice, once with $W = S$ and once with $W = T$, calculating functions $\mu^C(\cdot, S)$ and $\mu^C(\cdot, T)$, respectively. The RFC object $\hat{S}$ is simply defined as $\{c \in C\colon \mu^C(c,S) > \mu^C(c,T)\}$. Similarly, the RFC co-object $\hat{T} = \{c \in C\colon \mu^C(c,T) > \mu^C(c,S)\}$. Since $\mathrm{GC}_{\mathrm{max}}$ runs in a linear time with respect to the image size $|C|$, a fact theoretically proved in [6], this does not add much to a total run time of the algorithm, especially in comparison with the running time of the $\mathrm{GC}_{\mathrm{sum}}$ component, which runs in time of order $O(|C|^{2.5})$ or greater. We choose, as $\hat{S}$ and $\hat{T}$, the RFC objects rather than the IRFC objects—the standard output of $\mathrm{GC}_{\mathrm{max}}$—since they constitute the smallest objects in $\mathcal{X}_\infty(S,T)$ and $\mathcal{X}_\infty(T,S)$, respectively. In particular, these are the largest sets for which $\mathcal{X}_\infty(\hat{S},\hat{T}) = \mathcal{X}_\infty(S,T)$. This leaves extra room for the $\mathrm{GC}_{\mathrm{sum}}$ step of the algorithm to act upon, which chooses an object from $\mathcal{X}(\hat{S},\hat{T})$, while preserving the extrema choices, $\hat{S}$ and $\hat{T}$, indicated by $\mathrm{GC}_{\mathrm{max}}$.

We have the following two theorems, describing nice properties of $\mathrm{GC}_{\mathrm{sum}}^{\mathrm{max}}$. The first of these theorems immediately follows from the similar result on RFC segmentations.

**Theorem 3.1** *Let $I = \langle C, f\rangle$ be an image and $S, T \subset C$ non-empty disjoint sets of seeds. If the sets $S'$ and $T'$ have the same connected components, respectively, as those of $\hat{S}$ and $\hat{T}$, then $\mathrm{GC}_{\mathrm{sum}}^{\mathrm{max}}(I,S,T)$ and $\mathrm{GC}_{\mathrm{sum}}^{\mathrm{max}}(I,S',T')$ have identical outputs. In particular, if each of $\hat{S}$ and $\hat{T}$ has only one connected component in $G$, then any other choice of sets of seeds $S' \subset \hat{S}$ and $T' \subset \hat{T}$ leads to identical delineations.*

The above theorem describes the robustness of $\mathrm{GC}_{\mathrm{sum}}^{\mathrm{max}}$ with respect to the seed set size and location. The following theorem describes robustness of $\mathrm{GC}_{\mathrm{sum}}^{\mathrm{max}}$ with respect to remapping the image intensity by an increasing function, which depends on the way the weight/affinity function is created from the image intensity function.

**Theorem 3.2** *Let $I = \langle C, f\rangle$ and $I' = \langle C, f'\rangle$ be the images with associated weighted graphs $G = \langle V, E, w\rangle$ and $G' = \langle V, E, w'\rangle$, respectively. If $w'$ is a modification of $w$ via an increasing linear function (i.e., if $w'$ is a composition $L \circ w$ of $w$ and a linear function $L$), then for every seed sets $S, T \subset C$, the outputs of $\mathrm{GC}_{\mathrm{sum}}^{\mathrm{max}}(I,S,T)$ and $\mathrm{GC}_{\mathrm{sum}}^{\mathrm{max}}(I',S,T)$ are identical. More generally, if $w'$ is a modification of $w$ via an increasing function, then the associated RFC approximations $\langle \hat{S}, \hat{T}\rangle$ and $\langle \hat{S}', \hat{T}'\rangle$ are identical.*

Also, less formally, $\mathrm{GC}_{\mathrm{sum}}^{\mathrm{max}}$ has the following nice properties. Some level of *boundary smoothness* is assured for the output of $\mathrm{GC}_{\mathrm{sum}}^{\mathrm{max}}$ by a similar property of $\mathrm{GC}_{\mathrm{sum}}$. Similarly, some level of *leakage control* is achieved. The greater robustness (insensitivity) to the artifacts such as a *slow background variation* component modulating the image intensity function can be achieved by a careful creation of $w$.

## 4. EXPERIMENTAL RESULTS & CONCLUSION

In this section we present the accuracy results of experiments involving two 2D datasets, each composed of 40 real MR images of the foot.

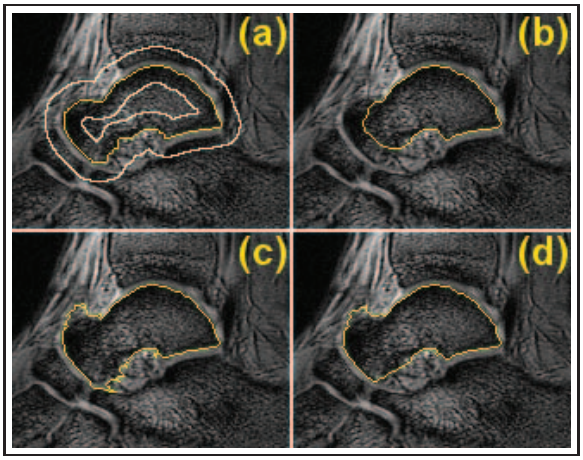


**Fig. 2**. (a) Ground truth of the talus (central contour), and example of seeds obtained by erosion (inner and outer contours). The corresponding results: (b) the result for $GC_{sum}$ (standard GC) algorithm, (c) the result for $GC_{max}$ (IRFC) algorithm, and (d) the result for $GC_{sum}^{max}$ (new RFC+GC) algorithm.

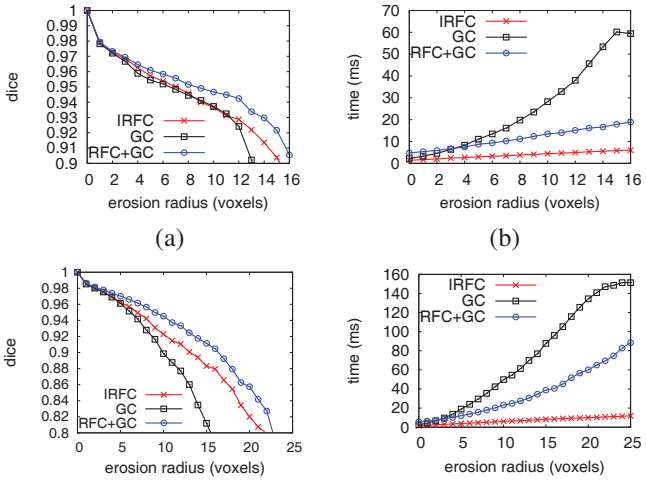


**Fig. 3**. (a-b) The mean accuracy and running time curves for segmenting talus by different algorithms; (c-d) The mean accuracy and running time curves for segmenting the calcaneus.

In the first experiment, we computed the mean performance curve for all the methods $GC_{sum}$ (i.e., standard GC), $GC_{max}$ (i.e., IRFC) and $GC_{sum}^{max}$ (i.e., RFC+GC) to segment the talus bone, for different seed sets obtained by eroding the ground truth, as shown in Fig 2(a). For the second dataset (not shown), we performed the segmentation of the calcaneus for all the methods. The arc weights $w(p,q)$ were computed as the complement of the difference of image intensities (i.e., as $K - |I(p) - I(q)|$, where $K$ stands for the maximum value of $|I(p) - I(q)|$, with $p, q \in C$).

Fig 2 shows some obtained results. The experimental curves are given in Fig 3, which show that the combined $GC_{sum}^{max}$ (i.e., RFC+GC) approach provided the best accuracy results in most cases. $GC_{sum}^{max}$ was also much more robust to seed quantity and position than $GC_{sum}$. This demonstrates that the combined approach can effectively work resulting in smooth boundaries, while $GC_{sum}$ alone fails under this setting because of the shrinking bias. In relation to running time, $GC_{sum}^{max}$ presented an intermediate performance as expected.

In conclusion, we have introduced an image segmentation algorithm $GC_{sum}^{max}$, which synergistically combines the strengths of two popular algorithms: $GC_{sum}$ and $GC_{max}$ (RFC). As future work, we intend to analyze other promising RFC extensions and to report its results in other image domains.

## 5. REFERENCES

[1] G. Aubert, L. Blanc-Féraud, "Some Remarks on the Equivalence between 2D and 3D Classical Snakes and Geodesic Active Contours," *IJCV* **34**(1) (1999), 19–28.

[2] J. Bioucas-Dias and G. Valadão, "Phase unwrapping via graph cuts," *IEEE TIP* **16**(3) (2007), 698–709.

[3] Y. Boykov, O. Veksler, R. Zabih, "Fast approximate energy minimization via graph cuts," *IEEE TPAMI* **23**(11) (2001), 1222–1239.

[4] K.C. Ciesielski, J.K. Udupa, "A framework for comparing different image segmentation methods and its use in studying equivalences between level set and fuzzy connectedness frameworks," *CVIU* **115** (2011), 721–734.

[5] K.C. Ciesielski, J.K. Udupa, A.X. Falcão, P.A.V. Miranda, "Comparison of fuzzy connectedness and graph cut segmentation algorithms," *Medical Imaging 2011: Image Processing, SPIE Proceedings 7962*, 2011.

[6] K.C. Ciesielski, J.K. Udupa, A.X. Falcão, P.A.V. Miranda, "Fuzzy Connectedness image segmentation in Graph Cut formulation: A linear-time algorithm and a comparative analysis," *J. Math. Imaging. Vis.*, in print.

[7] C. Couprie, L. Grady, L. Najman, H. Talbot, "Power Watersheds: A Unifying Graph-Based Optimization Framework," *IEEE TPAMI* **33**(7) (2011), 1384–1399.

[8] A.X. Falcão, J. Stolfi, R.A. Lotufo, "The image foresting transform: Theory, algorithms, and applications," *IEEE TPAMI* **26**(1) (2004), 19–29.

[9] H. Ishikawa, Exact optimization for Markov random fields with convex priors, *IEEE TPAMI* **25**(10) (2003), 1333–1336.

[10] V. Kolmogorov, R. Zabih, "What energy functions can be minimized via graph cuts," *IEEE TPAMI* **26**(2) (2004), 147–159.